HHS Public Access

Author manuscript

ACS Appl Bio Mater. Author manuscript; available in PMC 2022 June 21.

Published in final edited form as:

ACS Appl Bio Mater. 2021 June 21; 4(6): 5189–5200. doi:10.1021/acsabm.1c00369.

Sulfonate Hydrogel-siRNA Conjugate Facilitates Osteogenic Differentiation of Mesenchymal Stem Cells by Controlled Gene Silencing and Activation of BMP Signaling

Soyon Kim[1], **Jiabing Fan**[1], **Chung-Sung Lee**[1], **Chen Chen**[1], **Min Lee**[1,2,*]

[1]Division of Advanced Prosthodontics, University of California, Los Angeles, USA

[2]Department of Bioengineering, University of California, Los Angeles, USA

Abstract

Hydrogels have been widely used in bone tissue engineering due to their tunable characteristics that allow facile modifications with various biochemical properties to support cell growth and guide proper cell functions. Herein, we report a design of hydrogel-siRNA conjugate that facilitates osteogenesis via gene silencing and activation of bone morphogenetic protein (BMP) signaling. A sulfonate hydrogel is prepared by modifying chitosan with sulfoacetic acid to mimic a natural sulfated polysaccharide and to provide a hydrogel surface that enables BMP binding. Then, siRNA targeting noggin, an endogenous extracellular antagonist of BMP signaling, is covalently conjugated to the sulfonate hydrogel by visible blue light crosslinking. The sulfonate hydrogel-siRNA conjugate is efficient to bind BMPs and also successfully prolongs the release of siRNA for sustained noggin suppression, thereby resulting in significantly increased osteogenic differentiation. Lastly, demineralized bone matrix (DBM) is incorporated into the sulfonate hydrogel-siRNA conjugate, wherein the DBM incorporation induces noggin expression via a negative feedback mechanism that regulates BMP signaling in DBM. However, simultaneous delivery of siRNA downregulates noggin thus facilitating endogenous BMP activity and enhancing the osteogenic efficacy of DBM. These findings support a promising hydrogel RNA silencing platform for bone tissue engineering applications.

Keywords

hydrogel; siRNA; noggin; osteogenesis; bone tissue engineering

*Corresponding author: Min Lee, PhD, UCLA School of Dentistry, 10833 Le Conte Avenue, CHS 23-088F, Los Angeles, CA 90095-1668, leemin@ucla.edu, Phone: +1-310-825-6674, Fax: +1-310-825-6345.

Supporting Information

Primer information for qRT-PCR; Relative mineralization of DBM incorporated hydrogels with sulfoacetic acid and noggin siRNA conjugation at day 21; BMP-2 release and sequestering characterization of MC and SC hydrogels; 2D transfection experiments by collecting the releasates of siRNA from hydrogels at 3 h and 10 days and flow cytometry histogram; Relative cell growth and viability in hydrogels; BMP-2 release from DBM and DBM incorporation in hydrogels.

1. Introduction

Insufficient bone repair is a severe medical issue that is often derived from the skeletal defects or the accompanying complications. Autografting is considered as the gold standard for treating bone defects, but it cannot be extensively applied because of the limited supply with a high risk of infection and immune response[1]. Recent advances in bone tissue engineering provide various strategies for bone healing[2]. Specifically, biomaterial-based therapies stimulate endogenous bone regeneration with high quality control and low costs[3]. Hydrogels are widely used in bone tissue engineering because of their injectability, easy modifications and delivery potentials of various molecules[4]. Hydrogels mimicking bone extracellular matrix (ECM) could provide sites for cell attachment and calcium nucleation[5]. Hydrogels that had high binding affinities for osteogenic growth factors such as bone morphogenetic protein (BMP) were also verified to enhance osteogenesis[6]. Functionalization with heparin, a sulfated polysaccharide possessing notable binding affinity with BMP, could prolong protein delivery from hydrogel surfaces[7]. The strategy to adapt sulfate groups in hydrogels also supported BMP sequestering, stabilization, and osteogenesis[8, 9].

Despite high osteoinductivity of BMP, current BMP therapies demand supraphysiological concentrations due to the intrinsic instability of the protein, leading to adverse effects such as ectopic bone formation, swollen tissues, or cancer[10]. One alternative approach to augment BMP signaling is to enhance endogenous BMP activity by suppressing the expression of natural BMP antagonists such as noggin[11], gremlin[12], or chordin[13]. RNA interference (RNAi) is a powerful technique that can control gene expression, but it is very challenging to transport the negatively charged RNA molecules into the cells. Previous studies demonstrated that the delivery of noggin small interfering RNA (siRNA) via lentiviral[14] or liposomal[15] particles downregulated the gene expression and enhanced bone regeneration. However, gene transfer relying on viral vector can trigger immune, cytopathic responses, or unknown actions of other genes[16, 17]. Additionally, both viral and non-viral vectors have drawbacks such as off-targeting effects or fast clearance, requiring high dose or repeated injections[18, 19]. Many studies suggested the techniques to deliver genes without the carrier materials by functionalizing with cholesterol, methyl, methoxyethyl, or fluoro groups[20, 21]. These efforts successfully improved the cellular uptake and bioactivity of RNA in comparison to the naked one[22, 23].

Therefore, engineering hydrogels with carrier-free-RNA molecules provide great prospects in developing a hydrogel RNAi system[24]. The prevalent difficulties of carrier-based-delivery such as nonspecific targeting of the cells of interests or rapid diffusion can be modulated by the localized and controlled delivery of siRNA. The localized gene delivery could be accomplished by covalently conjugating siRNA to the network of bulk hydrogels[25]. Other studies showed that microRNA (miRNA) tethered hyaluronic acid hydrogels via hydrophobic interaction could deliver miRNA in a sustained manner[26]. Similar results were also found in siRNA tethered hydrogels, and the siRNA release profile could be triggered by bulk hydrogel erosion[27].

Furthermore, hydrogel-based therapy for bone repair can further make progress by incorporating currently available bone graft materials such as demineralized bone matrix (DBM) in the system. DBM naturally possessed many osteogenic growth factors, specifically BMPs. However, the bone formation capacity of DBM is less predictable and the bioactivities of BMPs released from DBM were easily compromised due to rapid degradation[28]. The BMPs present in DBM also induce the expression of BMP antagonists through a negative feedback mechanism to regulate excessive cellular exposure to BMPs, which potentially lowers the osteogenic effect of DBM. A recent study demonstrated that the use of DBM in combination with polymeric carriers could withhold, stabilize, and protect BMPs, resulting in the enhanced osteoinductivity[29].

In this study, a new hydrogel-siRNA conjugate is developed to enhance osteogenesis by guiding gene silencing and upregulating BMP signaling. The strategy to design a bioactive hydrogel was implemented by two-step-functionalization of methacrylate and sulfonate moieties. A methacrylate group enabled visible blue light-inducible crosslinking of hydrogel and sulfonate group allowed affinity binding with BMP-2 for longer retention of the protein and stimulation of the surrounding cells. Then, noggin siRNA was functionalized with disulfide-containing methacrylate group to be covalently conjugated to hydrogels. The strategy of localized delivery was achieved by covalent conjugation that effectively enhanced the initial incorporation and decreased the burst release of siRNA in a three-dimensional (3D) structure. Moreover, the hydrolysis of disulfide bonds between siRNA and hydrogels enabled release of siRNA over time. Lastly, DBM was incorporated in our hydrogel-siRNA conjugate to further induce osteogenic efficacy. The DBM-hydrogel composite was designed to deliver BMP-containing DBM in a localized manner. Moreover, it simultaneously downregulated noggin expression to maximize BMP pathway and osteogenesis. This strategy provided a new hydrogel RNAi platform with enhanced endogenous BMP signaling.

2. Experimental

2.1. Materials

Glycol chitosan (100 kDa), glycidyl methacrylate, riboflavin, sulfoacetic acid, 1-ethyl-3-(3-dimethylaminopropyl)-carbodiimide (EDC), *N*-hydroxysuccinimide (NHS), 1M MES buffer, dithiothreitol (DTT), pyridyl disulfide ethyl methacrylate (PDSEMA), dithiothreitol (DTT), hoechst 33342, L-ascorbic acid, β-glycerophosphate, dexamethasone, nitro blue tetrazolium (NBT), 5-bromo-4-chloro-3-indoxylphosphate (BCIP), *p*-nitrophenol phosphate, and alizarin red S were obtained from Sigma-Aldrich (St. Louis, MO). Recombinant human bone morphogenetic protein-2 (rhBMP-2) was provided from GenScript (Piscataway, NJ). Noggin siRNA was customized from Bioneer (Daejeon, Korea). Demineralized Bone Matrix (DBM) was supplied from MTF Biologics (Edison, NJ). A mouse bone marrow-derived stem cell line (BMSC), D1 ORL UVA [D1], was obtained from American Type Culture Collection (ATCC #CRL-12424, Manassas, VA). High glucose dulbecco's modified eagle's medium (DMEM), fetal bovine serum (FBS), antibiotic-antimycotic (AA), trypsin, neutral buffered formalin (NBF), calcein-AM, ethidium homodimer-1, Alexa Fluor 594 Phalloidin, TRIzol, cDNA transcription kit, Pierce BCA protein assay kit was purchased from Thermo Fisher

Scientific (Waltham, MA). Antibodies for western blot experiments were obtained from Santa Cruz Biotechnology and Millipore Sigma; GAPDH (sc-47724), noggin (sc-25656), mouse anti-rabbit IgG-HRP (sc-2357), m-IgGK BP-HRP (sc-516102), and p-Smad1/5/8 (AB3848-I). All reagents were utilized as received.

2.2. Preparation and Characterization of Hydrogels

Methacrylated glycol chitosan (MC) was synthesized by previously published method[30]. In brief, glycol chitosan was reacted with glycidyl methacrylate at 1:1 molar ratio to target amines at pH 9.0 for 40 h. Then, mixture was dialyzed against distilled water (DW), lyophilized, and rehydrated as 2% solution. Sulfoacetic acid chitosan (SC) was prepared by conjugating sulfoacetic acid to MC. Sulfoacetic acid, 2% MC in 0.1 M MES buffer, NHS, and EDC were reacted with 1:1:2:2 molar ratio to target amines at pH 6.5. Then the solution was purified in DW, lyophilized and rehydrated as 2% solution. The successful conjugation of sulfoacetic acid was confirmed by ^{1}H NMR in D_2O (Bruker ARX400) and fourier transform infrared spectrophotometer (FTIR, Jasco 420). Fabrication of hydrogel was performed by 40 s of visible blue light irradiation (400–500 nm, 300 mW cm^{-2}) with 6 μM riboflavin as a photointiator. The rheological properties of hydrogels were characterized by Discovery Hybrid Rheometers HR-3 (TA Instruments). The strain-sweep condition was 0.02 to 300% strain at a fixed 1.6 Hz frequency, and the frequency-sweep condition was 0.1 to 100 Hz frequency at γ = 5.0%. The compressive modulus of hydrogels was detected by 1.6 mm flat-end indentation test using Instron (Intron, Model 5564, Norwood, MA) with Poisson's ratio of 0.25[30]. The overall charge effect of sulfoacetic acid conjugation was confirmed by zeta potential measurement by Malvern Zetasizer Nano ZS. Then hydrogels were stained in 1% toluidine blue solution, washed in PBS, and imaged. Toluidine blue is a basic dye with high affinity for acidic substances such as sulfoacetic acid. BMP-2 binding affinity was measured by the previously published method[31]. In brief, hydrogels (50 μL) were incubated in 200 μL of rhBMP-2 solution (1–2000 ng mL^{-1}) for 1 h at room temperature to allow protein binding and washed in DW. After centrifugation at 4000 rpm, the supernatant was collected and quantified by BMP-2 ELISA kit (R&D Systems, MN). Then, BMP-2 was cultured in PBS or 2% hydrogel solution for 168h, and the change of BMP-2 concentration was measured to determine the effect of sulfoacetic acid conjugation on the half-life of BMP-2 (initially 100 ng mL^{-1})[29].

2.3. Methacrylation of RNA Oligonucleotides

Thiol modified RNA oligonucleotides is 5'-[Cholesterol]GAACAUCCAGACCCUAUCUt[FAM-dT][Thiol]-3'. The RNA oligonucleotide sequence information was obtained from the previously published noggin siRNA[15]. Negative control (non-targeting) RNA oligonucleotide (Ctrl siRNA) sequence was obtained from Bioneer. Thiol modified RNA oligonucleotides (5 OD) was activated by incubating in 1.0 N DTT for 15 min and extracted with ethyl acetate for 3 times. The 100 μM of activated oligonucleotides was reacted with 100 μM of PDSEMA at pH 2–3 for 3 h for methacrylation. Then the solution was purified and lyophilized. The quality and concentration of modified RNA is verified by NanoDrop (Thermo Fisher Scientific). The 260/280 value of unmodified RNA was 1.8 and modified RNA was 1.93. The 260/230 value

of unmodified RNA was 2.01 and modified RNA was 2.09. The 260/280 value near 2.0 and 260/230 in a range of 2.0–2.2 were considered as pure RNA.

2.4. Preparation of Hydrogel-siRNA Conjugate

Hydrogel solution, siRNA, and riboflavin were mixed and irradiated under visible blue light for 40 s to fabricate siRNA conjugated hydrogel. The final concentration of hydrogel is 2%, siRNA is 10 μM, and riboflavin is 6 μM. Then, 50 μL of hydrogels were washed in 500 μL of PBS for 10 min to measure the siRNA conjugation efficiency. Then, hydrogels were transferred to 500 μL of PBS and incubated for 14 days at 37 °C. The releasates was collected at the predetermined time points for quantification.

2.5. Cellular Uptake of siRNA in 3D Hydrogels

BMSCs obtained from ATCC were prepared by culturing in regular culture media with DMEM, 10% FBS, and 1% AA at 37 °C under 5% CO_2 humidified environment. Then, BMSCs were encapsulated in 100 μL of siRNA conjugated hydrogels at a concentration of 2×10^6 cells mL^{-1} and incubated in Opti-MEM, for 24 h and transferred to regular culture media. Cell-laden hydrogels were collected at day 1 and 10 for imaging and flow cytometry analysis. For imaging, hydrogels were fixed in 10% NBF for 15 min, washed, and stained with Hoechst 33342 and Alexa Fluor 594 phalloidin. Confocal SP8-STED/FLIM/FCS (Leica) microscope was used for three-channel imaging (blue, red, and green). For flow cytometry analysis, the collected hydrogels were incubated in 500 μL of 10 mg mL^{-1} lysozyme solution in PBS for 16 h to degrade the hydrogel network, and centrifuged at 1400 rpm to obtain cell pellets. The pellets were resuspended in 400 μL of PBS at 1×10^6 cells mL^{-1} concentration and cellular uptake efficiency was acquired by Digital Analyzers LSRII (IMED) flow cytometry (BD Biosciences).

2.6. Knockdown and Upregulation Efficiency in 3D Hydrogels

The hydrogels encapsulated with 2×10^6 cells mL^{-1} of BMSCs were collected at day 1, 5, 10, and 14 to evaluate *Noggin* knockdown and *BMP-2* upregulation efficiency. The quantitative real-time polymerase chain reaction (qRT-PCR) was used to examine gene expression. Total RNA was extracted from TRIzol and RNeasy mini kit (Qiagen), and reverse-transcribed using cDNA transcription kit. Then, qRT-PCR was performed with SYBR Green in LightCycler 480 PCR (Roche, IN). It was amplified for 45 cycles, and *GAPDH* was used for normalization. The primer information is provided in Supplementary Table 1.

2.7. Osteogenic Effect of siRNA Conjugated Hydrogels

50 μL of cell-laden hydrogels were initially incubated in Opti-MEM for 24 h and transferred to osteogenic media including regular culture media, 10 mM of *β*-glycerophosphate, 50 μg mL^{-1} of L-ascorbic acid, and 100 nM of dexamethasone for 14 days. At day 4, hydrogels were collected for alkaline phosphatase (ALP) staining and activity experiments. For ALP staining, hydrogels were fixed in 10% NBF for 15 min, and incubated in ALP solution including 100 mM Tris at pH 8.5, 50 mM $MgCl_2$, 100 mM NaCl, NBT, and BCIP for 2 h at room temperature. The stained hydrogels were imaged by Olympus SZX16

Stereomicroscope (Olympus, Japan). ALP activity was measured by using *p*-nitrophenol phosphate as a substrate. The collected hydrogels were digested in 0.02% Tween-20 solution in PBS, incubated with phosphate substrate for 10 min and an absorbance value was read at 405 nm. ALP activity value was normalized by total protein expression quantified by BCA protein assay. Mineralization was evaluated by staining of the fixed hydrogels in 2% alizarin red S staining and washing in PBS for 16 h. The stained hydrogels were imaged by Olympus SZX16 Stereomicroscope. Deposited calcium was quantified by colorimetric detection at 405 nm after acetic acid extraction and ammonium hydroxide neutralization. All values were normalized by the values from blank hydrogels without cells. Osteogenic gene expression was studied at two predetermined time points which were day 4 for *Runx2* and *ALP*, day 14 for *OCN*. The primer information can be found in Supplementary Table 1.

2.8. Preparation of DBM-Hydrogel Composites

DBM-hydrogel composite was formed by mixing DBM in SC hydrogels with various concentrations (0, 2, 4, 7, and 10%). Its incorporation in the hydrogel network was confirmed by scanning electron microscopy (SEM, Nova NanoSEM 230 microscope, FEI, OR). The compressive modulus of DBM-hydrogel composite was measured by Instron indentation method. BMSCs were encapsulated in DBM-hydrogel composites at a density of 2×10^6 cells mL^{-1} , cultured in Opti-MEM for 24 h, and moved to regular culture media for 14 days at 37 °C. The cell growth was quantified by PicoGreen assay (Thermo Fisher Scientific) at day 0, 1, 4, 7, and 14. The live and dead cells were shown by calcein-AM and ethidium homodimer-1 staining and cell viability was quantified by ImageJ (NIH, Bethesda, MD).

2.9. DBM-Hydrogel Composite Activating BMP Signaling and Osteogenesis

DBM-hydrogel composites were fabricated by visible light crosslinking with the final concentration of 7% DBM, 2% SC, 10 μM noggin siRNA, and 6 μM riboflavin. BMSCs were encapsulated with 2×10^6 cells mL^{-1} in the composites, cultured in Opti-MEM for 24 h and moved to osteogenic media for 14 days at 37 °C. ALP staining and activity tests were carried out at day 7, and alizarin red S staining and its quantification were performed at day 21. qRT-PCR was executed for *noggin*, *gremlin*, *chordin*, *BMP-2*, *Smad-5,* and *Id-1* on day 4, *Runx2*, *ALP,* and *OCN* at day 7 and 21. The primer information can be found in Supplementary Table 1.

2.10. Western Blot

Proteins were collected from BMSCs by RIPA buffer (EMD, Millipore, MA), and the concentration was assessed by BCA assay after culturing BMSCs on the surface of DBM-hydrogel composites for 72 hr. Protein samples were separated on 10% SDS-PAGE gel in Tris/glycine/SDS running buffer (Bio-Rad) under 90 V and 120 V at top and bottom gel respectively. Then, the proteins were transferred to the immobilization transfer membrane (Merck Millipore) at 250 V, 260 mA for 2 h. The membrane was blocked by 5% non-fat milk at 4 °C overnight and washed with 0.1% tween-20 solution in PBS. The membrane was incubated with primary antibodies against Noggin, pSmad 1/5/8, and GAPDH (Santa Cruz Biotechnology, 5000:1 dilution) for 2 h, and incubated with secondary antibodies for 1 h at room temperature. The signal was detected by the Clarity Western ECL substrate (Bio-Rad)

and the images were obtained by ImageLab (Bio-Rad). The images were further quantified by ImageJ (NIH, Bethesda, MD).

2.11. Statistical Analysis

Statistical analysis was performed using the Prism software. Statistical significance was evaluated by one- or two-way analysis of variance with Tukey's post hoc test, and a value of $p < 0.05$ was considered as statistically significant.

3. Results

3.1. Characterization of Hydrogels

Photocrosslinkable methacrylated chitosan (MC) and sulfonated chitosan (SC) hydrogel solutions were prepared by step-by-step substitution of primary amines in glycidyl chitosan backbone with glycidyl methacrylate and sulfoacetic acid (Figure 1a). ^{1}H NMR spectra (Figure 1b) confirmed the successful incorporation of methacrylate group (δ = 5.65 and 6.05 ppm, 32.7%)[30] and sulfonate group (δ = 1.87 ppm, 9.5%)[32]. FTIR results (Figure 1c) also verified the substitution by exhibiting C=C stretching at 1650 cm^{-1} and sulfonates at 1180 cm^{-1} wavenumber[33]. The rheological properties of MC and SC hydrogels were evaluated by monitoring the change of storage (G') and loss (G") modulus on strain-and frequency-sweep screening (Figure 1d). The strain sweep measurements displayed higher G' than G" for both MC and SC hydrogels, indicating viscoelastic gel-like features. The value of G' became lower than that of G" at higher strain, indicating destruction of the hydrogels with liquid-like behavior. The gel-like behavior of MC and SC hydrogels was well retained over a wide range of angular frequency. The compressive modulus of both hydrogels also exhibited similar values of 7.83 and 7.08 (Figure 1e). Both MC and SC hydrogels did not exhibit significant differences in mechanical properties. However, their notable differences in electrostatic potential was demonstrated by zeta potential and toluidine blue staining. The zeta potential values were +5.5 mV for MC and −4.3 mV for SC. Therefore, the surface of SC hydrogel was more acidic than MC, which made it more favorable to the basic dyes such as toluidine blue (Figure 1f). Then, the binding affinity of rhBMP-2, a basic protein with an isoelectric point near 8.5, on the hydrogel surface was empirically measured (Figure 1g). The BMP-2 binding on MC and SC hydrogels were indistinguishable below 50 ng mL^{-1} of BMP-2 possibly due to nonspecific binding[31], but it gradually changed that SC hydrogel revealed significantly higher binding affinity above 100 ng mL^{-1} of BMP-2 in comparison to MC hydrogel. The higher intermolecular interactions between BMP-2 and SC hydrogel solutions also extended the half-life of BMP-2 in comparison to MC hydrogel solution, indicating that SC is efficient to enhance stability of BMP-2 (Figure 1h).

3.2. siRNA Conjugation on Hydrogels

Noggin siRNA functionalized with thiol and cholesterol was modified with a methacrylate group to be ready to use in a photocrosslinking system (Figure 2a). Two siRNA incorporated hydrogels, without and with methacrylation, were prepared to evaluate the tethering efficiency of methacrylated siRNA. Noggin siRNA was incorporated into sulfonated chitosan hydrogels by simple mixing (Mix) or chemical conjugation (Conjugate) (Figure 2b). The initial incorporation ratio of siRNA in hydrogel network was 72.7% for the simple

mix group, while it was 95.3% for the conjugation group, indicating that the methacrylation of siRNA significantly improved the binding efficiency of siRNA in the photocrosslinkable hydrogel (Figure 2c). The long-term release of siRNA in the conjugated hydrogel was prolonged for 14 days in PBS in comparison to the high burst release of siRNA in the simple mix hydrogel (Figure 2d). siRNA was released out 70% after one day in the simple mix group, while the conjugated group exhibited only 24%. The siRNA release profile was not significantly changed in the presence of serum.

3.3. Cellular Uptake of siRNA in 3D Hydrogels

The long-term siRNA uptake in 3D culture system was investigated by confocal microscope imaging and flow cytometry analysis. FAM-functionalization was used to track siRNA with green fluorescence. Cholesterol-functionalization of siRNA could make it enter the cell membrane without additional vector materials[22, 23]. The successful uptake of siRNA was monitored at day 1 in both mix and conjugate groups; however, siRNA was not observed in the mix group at day 10 (Figure 3a). This result was consistent with the siRNA release profile (Figure 2d) that the majority of siRNA did not remain in the simple mix group at day 10. The quantified result of cellular uptake was analyzed by flow cytometry (Figure 3b). Both of the groups at day 1 showed similar uptake efficiency of 64.0% for the mix and 65.3% for the conjugate. In spite of the comparable initial cellular uptake, it changed significantly at day 10 that almost no uptake was found for the mix group, but 26.9% for the conjugate group. Therefore, the siRNA conjugated hydrogel system successfully supported the long-term cellular uptake in the 3D system.

3.4. Knockdown and Upregulation Efficiency in 3D Hydrogels

After confirming the long-term cellular uptake, we investigated how long the transfection was effective in the 3D hydrogel environment by comparing three groups; sulfonated chitosan hydrogels without noggin siRNA (blank), with simple mixing of noggin siRNA (mix), with chemical conjugation of noggin siRNA (conjugate). Significant suppression of noggin was observed by qRT-PCR in both groups at day 1, 68% for the mix group and 72% for the conjugate group compared with the blank group (Figure 4a). Knockdown efficiency of the mix group lessened from day 5 and was not significantly different from the blank group, while the conjugate group was able to maintain effective knockdown efficiency until day 14. Noggin suppression was also effective to modulate BMP-2 gene expression (Figure 4b). Endogenous BMP activity is expected to remain unhindered by the knockdown of noggin, resulting in a positive feedback loop on BMP expression levels. Both mix and conjugate groups exhibited approximately 1.5-fold increment in BMP-2 expression at day 1. However, the mix group was not able to continue upregulating BMP-2 expression after the first day of siRNA administration, while the conjugate group could effectively upregulate BMP-2 expression until day 10. These results indicated that the conjugate model had longer gene suppression ability compared with the mix system.

3.5. Osteogenic Effect of siRNA Conjugated Hydrogels

We studied whether higher noggin suppression of siRNA conjugation in 3D sulfonate hydrogel system could influence the osteogenic gene expression (Figure 5a) and further osteogenesis. The early osteogenic markers, *Runx2* and *ALP*, were both upregulated at day

4 with sulfonate modification (SC and SCNog) as well as siRNA conjugation (MCNog and SCNog). The late and more specific osteogenic marker, *OCN*, was also increased at day 14 with sulfonate and siRNA functionalization. Previous studies also demonstrated that sulfonate incorporated composite-hydrogel[8] could enhance *Runx2*, *ALP*, and *OCN*. Knockdown of *noggin* via liposomal delivery[15] could also increase the expression of these osteogenic genes by ~1.5-fold. It indicated that both sulfonate and siRNA conjugation could effectively enhance osteogenic gene expression. ALP and alizarin red S staining were performed to measure ALP and mineral deposition in hydrogel (Figure 5b). The stronger staining in ALP and mineral production were observed with the incorporation of sulfonate and siRNA in hydrogels, demonstrating that the dual functionalization successfully improved osteogenesis.

3.6. Characterization of DBM-Hydrogel Composites

Hydrogel is an effective carrier for DBM to protect the undesired dispersion by body fluid potentially leading to ectopic bone formation and lowering the localized osteogenic effect[34]. SC hydrogels enabled homogenous integration of DBM up to 10% concentration as confirmed by macroscopic observation (Figure 6a). The size distribution of DBM is 0.212–0.850 mm and the microscale interphase of DBM. Hydrogel network stably covered DBM particles after the composite formation, which was confirmed in SEM images (Figure 6b). DBM incorporation in hydrogels escalated the compressive modulus at 2 and 7% points indicating no difference in 2–4% and 7–10% ranges (Figure 6c). DBM also provided bone matrix molecules, such as type I collagen and its derivatives, which was beneficial to the attachment and growth of the cells[35]. The rate of BMSC proliferation was significantly higher in the DBM-hydrogel composites in comparison to blank hydrogel groups at day 14 as determined using a DNA content assay (Figure 6d). Combined with the mechanical properties and cell growth results, 7% DBM-hydrogel composite was selected as an optimal concentration for further studies, which was also comparable to the commercial DBM-polymer products[36].

3.7. DBM-Hydrogel Composite Activating BMP Signaling and Osteogenesis

The augmented osteogenesis was observed with DBM incorporation (SCCtrl+DBM and SCNog+DBM) and noggin suppression (SCNog and SCNog+DBM). DBM is a natural reservoir of BMP-2, the essential osteoinductive growth factor, and noggin is a distinctive antagonist of BMP-2. The combination of two strategies, DBM incorporation and noggin knockdown, could potentially activate BMP signaling and enhance osteogenesis. The mechanism was investigated by analyzing the expression of the related genes (Figure 7a) and proteins (Figure 7b). Hydrogel-siRNA conjugate, SCNog, effectively suppressed noggin expression regardless of DBM existence. In addition, noggin suppression strategy did not cause a compensatory effect of other BMP antagonists such as *gremlin* and *chordin*. Similar results were also found in another noggin downregulation strategy using lipid nanoparticles[37]. The expression levels of *BMP-2*, *Smad-5*, and *Id-1* were higher in SC hydrogels with DBM incorporation and noggin suppression compared with the groups incorporating DBM or siRNA alone, suggesting significantly enhanced BMP/Smad signaling pathway by DBM and noggin knockdown. Consequently, early osteogenic gene markers such as *Runx2* and *ALP* were upregulated at day 7, while *OCN* was more

significantly upregulated during the late stages of osteogenic differentiation at day 21. Lastly, noggin and pSmad 1/5/8 protein expression was evaluated by western blot and the results showed enhanced pSmad 1/5/8 and decreased noggin expression in SCNog hydrogels containing DBM. These findings indicate that the cooperative strategy of DBM treatment, along with noggin suppression, could effectively trigger BMP signaling pathway. In addition, strong mineral deposition was confirmed in BMSCs encapsulated in DBM-hydrogel composites with noggin suppression, and the amount of mineral deposition was much greater in SC hydrogels (Figure S1).

4. Discussion

Although cell- or growth factor-based approaches could effectively support bone regeneration, their utilization is limited due to the restricted supply and potential adverse effects. It is well known to use recombinant human BMP-2 (rhBMP-2) in clinical bone applications, but the commercial collagen carrier was not suitable for the sustained delivery due to the high burst release[38]. Therefore, high dose administration was required for the conventional rhBMP-2 treatment and it led to undesired adipogenesis or osteoclastic activity[10]. In this work, we have used sulfoacetic acid to modify hydrogel surface to mimic a natural sulfated polysaccharide in ECM, heparin. Heparin forms a stable interconnected structure with BMPs[39] to act as a catalyst of signaling and controls the activities of BMPs by regulating noggin diffusion[40, 41]. In addition, synthetic heparin mimetics incorporating sulfate or sulfonate groups were widely designed and proven to possess similar bioactivities with heparin[8, 42, 43]. The ability of sulfated polysaccharides to stabilize BMP-2 activity has been demonstrated in our recent proof-of-concept study[8, 29] by incorporating heparin or heparin-mimicking polysulfonates into MeGC hydrogels. However, the direct use of heparin is limited by its heterogeneity and unwanted side effects[44–46]. Moreover, synthetic heparin mimics have been physically combined with hydrogels, which can easily dissociate and disperse in vivo. In the current study, we have chemically conjugated sulfoacetic acid into MeGC hydrogels. We have used diverse concentrations of sulfoacetic acid (0.1–2 molar ratio to MC), and both SC1 and SC2 have shown the significant lowering of rhBMP-2 burst release in comparison to MC and SC0.5 (Figure S2a). However, both SC1 and SC2 did not exhibit differences, so we have selected SC1 for further experiments. The sulfonate hydrogel delayed rhBMP-2 release profile for 14 days (Figure S2b). It also effectively sequestered both exogenous rhBMP-2 and cell-secreted endogenous BMP-2 (Figure S2c). These results are similar to those reported in our previous studies using hydrogels modified with heparin or heparin-mimicking polysulfonates. The observed increased BMP-2 binding and sustained release can be attributed to the negative zeta potential of SC hydrogels (−4.3 mV) similar to our previous heparinized (−3 mV) or polysulfonated hydrogels (−2 to −8 mV). Collectively, BMP-2 binds to the sulfonate hydrogel, which modulates release and sequestering of BMP-2.

A disulfide-containing methacrylated siRNA enabled covalent conjugation on sulfonate hydrogel via photocrosslinking as well as the sustained release through the hydrolysis of disulfide bonds over time. Our new sulfonate hydrogel-siRNA conjugate successfully transported siRNA into the cells in 3D system for 10 days. We have conducted 2d transfection experiments by collecting the releasates of siRNA from hydrogels at 3 h and 10

days (Figure S3). The transfection efficiency results were similar with the 3D system that the highest was around 65%. Cholesterol-only-mediated gene uptake was not high enough in comparison to lipofectamine-mediated uptake. However, the siRNA uptake efficiency could be further enhanced with additional lipophilic modifications like long-chain fatty acids or bile acids in addition to cholesterol[47].

A visible blue light crosslinkable MC hydrogel platform with riboflavin initiator was validated for high biocompatibility contributing favorable cell growth[30]. However, modification of MC hydrogel could alter its microenvironment, so we have evaluated the biocompatibility of sulfonate hydrogel-siRNA conjugate, SCNog. The conjugation of sulfonate group and siRNA to MC hydrogels did not change the cell metabolic activity for 14 days (Figure S4a). It also maintained the viability of the encapsulated cells above 90% for 14 days (Figure S4b), which demonstrated that the sulfonate hydrogel-siRNA conjugate still provided a cell-favorable microenvironment.

Moreover, sulfonate hydrogels enhanced the osteogenic differentiation of the encapsulated mesenchymal stem cells compared with unmodified hydrogels. The increased osteogenesis is likely due to SC-mediated sequestration of cell-secreted BMP-2 as confirmed by immunostaining for BMP-2. These results were consistent with our previous findings observed in the hydrogels modified with heparin or heparin-mimicking polysulfonate[8], indicating the ability of SC to bind BMP-2 similar to heparin. In addition, the potency of SC hydrogels could be further enhanced by inhibiting expression of BMP antagonists such as noggin. The current study demonstrated that delivery of noggin siRNA in SC hydrogels induced significantly higher osteogenesis compared with our previous heparinized or polysulfonated hydrogels without noggin suppression. This data suggests a promising sulfate hydrogel-siRNA conjugate to augment BMP pathway and bone regeneration.

DBM is a promising allogenic bone graft widely used in bone surgery[48]. DBM contains many osteoinductive growth factors such as BMP-2, which became more accessible with the demineralization process[49]. BMP-2 is the most abundant osteoinductive growth factor in DBM, and it is released from DBM over time (Figure S5a). However, the released growth factors of DBM are easily exposed to the physiologically stressed conditions, resulting in the loss of bioactivities[50]. Our sulfonate hydrogel-siRNA conjugate can be an effective candidate carrier of DBM by sequestering the released cytokines, suppressing the noggin expression, and localizing the DBM particles. In response to BMPs, cells express BMP antagonists such as noggin in an auto-inhibitory manner to reduce the increased level of endogenous BMP signaling[51]. The qualitative morphology of DBM in the composite was observed by the stained H&E cryosection images (Figure S5b). In addition, the image of picrosirius staining exhibited abundant collagen in DBM particles. We also observed a compensatory effect of noggin after the incorporation of DBM, supporting the existence of BMP released from DBM. Therefore, BMP antagonism is one reason to reduce the osteogenic efficacy of conventional DBM. Our sulfonate hydrogel-siRNA enabled the regulation of noggin over time. Taken together, regulation of noggin via sulfonate hydrogel-siRNA carrier for DBM incorporation is a promising strategy to improve overall osteogenic efficacy of DBM.

Building on our prior work, the current study chemically conjugates sulfoacetic acid into MeGC hydrogels with siRNA delivery and further delineates the molecular mechanisms involved in enhanced osteogenesis mediated by the hydrogel-DBM composite. Future study will evaluate the efficiency of the hydrogel composite system to promote bone regeneration in an animal model. Various BMP antagonists are expressed during the different stages of bone regeneration process. Although our hydrogel system did not significantly upregulate chordin or gremlin in BMSCs, noggin blockage could result in compensatory increases in other BMP antagonists *in vivo*. Our hydrogel-siRNA conjugate platform can easily deliver multiple siRNAs, which potentially overcome these issues. Moreover, the degradation rate of bulk hydrogels can be modulated to facilitate infiltration of endogenous cells or to accelerate siRNA release. Lastly, our hydrogel could be an appropriate carrier for BMP-2 improve current rhBMP therapies with a reduced dose required for bone regeneration.

5. Conclusion

We have designed a new sulfonate hydrogel-siRNA conjugate facilitating osteogenic differentiation. Hydrogel modified with both sulfonate and methacrylate groups enabled the enhanced binding affinity of BMP and covalent tethering of siRNA by visible blue light crosslinking. The covalent conjugation of siRNA prolonged release, cellular uptake, and gene silencing over time, resulting in the enhanced osteogenesis. The incorporation of DBM in hydrogel could further improve its osteogenic efficacy by activating BMP signaling. These results demonstrate that our hydrogel-siRNA conjugate provides a foundation of promising hydrogel RNAi system and biomaterial-based therapy for tissue engineering.

Supplementary Material

Refer to Web version on PubMed Central for supplementary material.

Acknowledgements

This research was supported by grants from the National Institutes of Health (R01 DE027332), the Department of Defense (W81XWH-18-1-0337), and the MTF Biologics. The flow cytometry core at UCLA was supported by National Institutes of Health awards P30 CA016042 and 5P30 AI028697, and by the Jonsson Comprehensive Cancer Center, the UCLA AIDS Institute, the David Geffen School of Medicine at UCLA, the UCLA Chancellor's Office, and the UCLA Vice Chancellor's Office of Research.

References

1. Pape HC; Evans A; Kobbe P, Autologous Bone Graft: Properties and Techniques. J Orthop Trauma 2010, 24 Suppl 1, S36–40. [PubMed: 20182233]
2. Kneser U; Schaefer DJ; Polykandriotis E; Horch RE, Tissue Engineering of Bone: the Reconstructive Surgeon's Point of View. Journal of Cellular and Molecular Medicine 2006, 10 (1), 7–19. [PubMed: 16563218]
3. Moroni L; Nandakumar A; Barrere-de Groot F; van Blitterswijk CA; Habibovic P, Plug and Play: Combining Materials and Technologies to Improve Bone Regenerative Strategies. Journal of Tissue Engineering and Regenerative Medicine 2015, 9 (7), 745–759. [PubMed: 23671062]
4. Gibbs DM; Black CR; Dawson JI; Oreffo RO, A Review of Hydrogel Use in Fracture Healing and Bone Regeneration. J Tissue Eng Regen Med 2016, 10 (3), 187–98. [PubMed: 25491789]

5. Kim S; Cui ZK; Fan JB; Fartash A; Aghaloo TL; Lee M, Photocrosslinkable Chitosan Hydrogels Functionalized with the RGD Peptide and Phosphoserine to Enhance Osteogenesis. Journal of Materials Chemistry B 2016, 4 (31), 5289–5298. [PubMed: 28044100]
6. Bai X; Gao M; Syed S; Zhuang J; Xu X; Zhang XQ, Bioactive Hydrogels for Bone Regeneration. Bioact Mater 2018, 3 (4), 401–417. [PubMed: 30003179]
7. Kisiel M; Klar AS; Ventura M; Buijs J; Mafina MK; Cool SM; Hilborn J, Complexation and Sequestration of BMP-2 from an ECM Mimetic Hyaluronan Gel for Improved Bone Formation. Plos One 2013, 8 (10), e78551. [PubMed: 24167632]
8. Kim S; Cui ZK; Kim PJ; Jung LY; Lee M, Design of Hydrogels to Stabilize and Enhance Bone Morphogenetic Protein Activity by Heparin Mimetics. Acta Biomater 2018, 72, 45–54. [PubMed: 29597024]
9. Peschel D; Zhang K; Fischer S; Groth T, Modulation of Osteogenic Activity of BMP-2 by Cellulose and Chitosan Derivatives. Acta Biomater 2012, 8 (1), 183–93. [PubMed: 21884830]
10. James AW; LaChaud G; Shen J; Asatrian G; Nguyen V; Zhang XL; Ting K; Soo C, A Review of the Clinical Side Effects of Bone Morphogenetic Protein-2. Tissue Engineering Part B-Reviews 2016, 22 (4), 284–297. [PubMed: 26857241]
11. Fan J; Im CS; Guo M; Cui Z-K; Fartash A; Kim S; Patel N; Bezouglaia O; Wu BM; Wang C-Y; Aghaloo TL; Lee M, Enhanced Osteogenesis of Adipose-Derived Stem Cells by Regulating Bone Morphogenetic Protein Signaling Antagonists and Agonists. Stem Cells Translational Medicine 2016, 5 (4), 539–551. [PubMed: 26956209]
12. Hu K; Sun H; Gui B; Sui C, Gremlin-1 Suppression Increases BMP-2-Induced Osteogenesis of Human Mesenchymal Stem Cells. Mol Med Rep 2017, 15 (4), 2186–2194. [PubMed: 28260028]
13. Kwong FN; Richardson SM; Evans CH, Chordin Knockdown Enhances the Osteogenic Differentiation of Human Mesenchymal Stem Cells. Arthritis Res Ther 2008, 10 (3), R65. [PubMed: 18533030]
14. Fan J; Park H; Tan S; Lee M, Enhanced Osteogenesis of Adipose Derived Stem Cells with Noggin Suppression and Delivery of BMP-2. PLoS One 2013, 8 (8), e72474. [PubMed: 23977305]
15. Cui Z-K; Fan J; Kim S; Bezouglaia O; Fartash A; Wu BM; Aghaloo T; Lee M, Delivery of siRNA via Cationic Sterosomes to Enhance Osteogenic Differentiation of Mesenchymal Stem Cells. Journal of Controlled Release 2015, 217, 42–52. [PubMed: 26302903]
16. Waehler R; Russell SJ; Curiel DT, Engineering Targeted Viral Vectors for Gene Therapy. Nature Reviews Genetics 2007, 8 (8), 573–587.
17. Bouard D; Alazard-Dany N; Cosset FL, Viral Vectors: From Virology To Transgene Expression. British Journal of Pharmacology 2009, 157 (2), 153–165. [PubMed: 18776913]
18. Tamura A; Nagasaki Y, Smart siRNA Delivery Systems Based on Polymeric Nanoassemblies and Nanoparticles. 2010, 5 (7), 1089–102.
19. Xue HY; Liu S; Wong HL, Nanotoxicity: A Key Obstacle to Clinical Translation of siRNA-Based Nanomedicine. Nanomedicine (Lond) 2014, 9 (2), 295–312. [PubMed: 24552562]
20. Dovydenko I; Tarassov I; Venyaminova A; Entelis N, Method of Carrier-Free Delivery of Therapeutic RNA Importable into Human Mitochondria: Lipophilic Conjugates with Cleavable Bonds. Biomaterials 2016, 76, 408–17. [PubMed: 26561937]
21. Zheng Y; Tai W, Insight into the siRNA Transmembrane Delivery—From Cholesterol Conjugating to Tagging. WIREs Nanomedicine and Nanobiotechnology 2020, 12 (3), e1606. [PubMed: 31788983]
22. Hassler MR; Turanov AA; Alterman JF; Haraszti RA; Coles AH; Osborn MF; Echeverria D; Nikan M; Salomon WE; Roux L; Godinho BMDC; Davis SM; Morrissey DV; Zamore PD; Karumanchi SA; Moore MJ; Aronin N; Khvorova A, Comparison of Partially and Fully Chemically-Modified siRNA in Conjugate-Mediated Delivery In Vivo. Nucleic Acids Res 2018, 46 (5), 2185–2196. [PubMed: 29432571]
23. Bienk K; Hvam ML; Pakula MM; Dagnæs-Hansen F; Wengel J; Malle BM; Kragh-Hansen U; Cameron J; Bukrinski JT; Howard KA, An Albumin-Mediated Cholesterol Design-Based Strategy for Tuning siRNA Pharmacokinetics and Gene Silencing. J Control Release 2016, 232, 143–51. [PubMed: 27084489]

24. Wang LL; Burdick JA, Engineered Hydrogels for Local and Sustained Delivery of RNA-Interference Therapies. Advanced Healthcare Materials 2017, 6 (1), 1601041.
25. Nguyen MK; Huynh CT; Gilewski A; Wilner SE; Maier KE; Kwon N; Levy M; Alsberg E, Covalently Tethering siRNA to Hydrogels for Localized, Controlled Release and Gene Silencing. Sci Adv 2019, 5 (8), eaax0801. [PubMed: 31489374]
26. Wang LL; Liu Y; Chung JJ; Wang T; Gaffey AC; Lu M; Cavanaugh CA; Zhou S; Kanade R; Atluri P; Morrisey EE; Burdick JA, Sustained miRNA Delivery From An Injectable Hydrogel Promotes Cardiomyocyte Proliferation And Functional Regeneration After Ischaemic Injury. Nature Biomedical Engineering 2017, 1 (12), 983–992.
27. Wang LL; Chung JJ; Li EC; Uman S; Atluri P; Burdick JA, Injectable and Protease-Degradable Hydrogel for siRNA Sequestration and Triggered Delivery to the Heart. Journal of Controlled Release 2018, 285, 152–161. [PubMed: 29981357]
28. Chesmel KD; Branger J; Wertheim H; Scarborough N, Healing Response to Various Forms of Human Demineralized Bone Matrix in Athymic Rat Cranial Defects. J Oral Maxillofac Surg 1998, 56 (7), 857–63; discussion 864–5. [PubMed: 9663577]
29. Kim S; Fan J; Lee C-S; Chen C; Bubukina K; Lee M, Heparinized Chitosan Stabilizes the Bioactivity of BMP-2 and Potentiates the Osteogenic Efficacy of Demineralized Bone Matrix. Journal of Biological Engineering 2020, 14 (1), 6. [PubMed: 32165922]
30. Hu J; Hou Y; Park H; Choi B; Hou S; Chung A; Lee M, Visible Light Crosslinkable Chitosan Hydrogels for Tissue Engineering. Acta Biomater 2012, 8 (5), 1730–1738. [PubMed: 22330279]
31. EL-Sharif HF; Hawkins DM; Stevenson D; Reddy SM, Determination of Protein Binding Affinities within Hydrogel-Based Molecularly Imprinted Polymers (HydroMIPs). Phys Chem Chem Phys 2014, 16 (29), 15483–9. [PubMed: 24950144]
32. Carnachan SM; Hinkley SFR, Heparan Sulfate Identification and Characterisation: Method I. Heparan Sulfate Identification by NMR Analysis. Bio-protocol 2017, 7 (7), e2196. [PubMed: 34541207]
33. Coates J, Interpretation of Infrared Spectra, A Practical Approach. Encyclopedia of Analytical Chemistry 2006, 1–23.
34. Shehadi JA; Elzein SM, Review of Commercially Available Demineralized Bone Matrix Products for Spinal Fusions: A Selection Paradigm. Surg Neurol Int 2017, 8, 203. [PubMed: 28904830]
35. Chen B; Lin H; Wang J; Zhao Y; Wang B; Zhao W; Sun W; Dai J, Homogeneous Osteogenesis and Bone Regeneration by Demineralized Bone Matrix Loading with Collagen-Targeting Bone Morphogenetic Protein-2. Biomaterials 2007, 28 (6), 1027–35. [PubMed: 17095085]
36. Zhang H; Yang L; Yang XG; Wang F; Feng JT; Hua KC; Li Q; Hu YC, Demineralized Bone Matrix Carriers and their Clinical Applications: An Overview. Orthop Surg 2019, 11 (5), 725–737. [PubMed: 31496049]
37. Ghadakzadeh S; Hamdy RC; Tabrizian M, Efficient In Vitro Delivery of Noggin siRNA Enhances Osteoblastogenesis. Heliyon 2017, 3 (11), e00450. [PubMed: 29167826]
38. McKay WF; Peckham SM; Badura JM, A Comprehensive Clinical Review of Recombinant Human Bone Morphogenetic Protein-2 (INFUSE (R) Bone Graft). International Orthopaedics 2007, 31 (6), 729–734. [PubMed: 17639384]
39. Takada T; Katagiri T; Ifuku M; Morimura N; Kobayashi M; Hasegawa K; Ogamo A; Kamijo R, Sulfated Polysaccharides Enhance the Biological Activities of Bone Morphogenetic Proteins. J Biol Chem 2003, 278 (44), 43229–35. [PubMed: 12912996]
40. Paine-Saunders S; Viviano BL; Economides AN; Saunders S, Heparan Sulfate Proteoglycans Retain Noggin at the Cell Surface: a Potential Mechanism for Shaping Bone Morphogenetic Protein Gradients. J Biol Chem 2002, 277 (3), 2089–96. [PubMed: 11706034]
41. Zhao BH; Katagiri T; Toyoda H; Takada T; Yanai T; Fukuda T; Chung UI; Koike T; Takaoka K; Kamijo R, Heparin Potentiates the In Vivo Ectopic Bone Formation Induced by Bone Morphogenetic Protein-2. Journal of Biological Chemistry 2006, 281 (32), 23246–23253.
42. Paluck SJ; Nguyen TH; Lee JP; Maynard HD, A Heparin-Mimicking Block Copolymer Both Stabilizes and Increases the Activity of Fibroblast Growth Factor 2 (FGF2). Biomacromolecules 2016, 17 (10), 3386–3395. [PubMed: 27580376]

43. Nguyen TH; Kim SH; Decker CG; Wong DY; Loo JA; Maynard HD, A Heparin-Mimicking Polymer Conjugate Stabilizes Basic Fibroblast Growth Factor. Nature Chemistry 2013, 5 (3), 221–227.
44. Mulloy B; Forster MJ, Conformation and Dynamics of Heparin and Heparan Sulfate. Glycobiology 2000, 10 (11), 1147–56. [PubMed: 11087707]
45. Battistelli S; Genovese A; Gori T, Heparin-Induced Thrombocytopenia in Surgical Patients. Am J Surg 2010, 199 (1), 43–51. [PubMed: 20103065]
46. Schindewolf M; Lindhoff-Last E; Ludwig RJ; Boehncke WH, Heparin-Induced Skin Lesions. Lancet 2012, 380 (9856), 1867–79. [PubMed: 22642893]
47. Wolfrum C; Shi S; Jayaprakash KN; Jayaraman M; Wang G; Pandey RK; Rajeev KG; Nakayama T; Charrise K; Ndungo EM; Zimmermann T; Koteliansky V; Manoharan M; Stoffel M, Mechanisms and Optimization of In Vivo Delivery of Lipophilic siRNAs. Nature Biotechnology 2007, 25 (10), 1149–1157.
48. Kuhls R; Werner-Rustner M; Küchler I; Soost F, Human Demineralised Bone Matrix as a Bone Substitute for Reconstruction of Cystic Defects of the Lower Jaw. Cell Tissue Bank 2001, 2 (3), 143–53. [PubMed: 15256912]
49. Wildemann B; Kadow-Romacker A; Haas NP; Schmidmaier G, Quantification of Various Growth Factors in Different Demineralized Bone Matrix Preparations. J Biomed Mater Res A 2007, 81 (2), 437–42. [PubMed: 17117475]
50. Haddad AJ; Peel SAF; Clokie CML; Sandor GKB, Closure of Rabbit Calvarial Critical-Sized Defects Using Protective Composite Allogeneic and Alloplastic Bone Substitutes. Journal of Craniofacial Surgery 2006, 17 (5), 926–934.
51. Gazzerro E; Gangji V; Canalis E, Bone Morphogenetic Proteins Induce the Expression of Noggin, Which Limits Their Activity in Cultured Rat Osteoblasts. J Clin Invest 1998, 102 (12), 2106–14. [PubMed: 9854046]

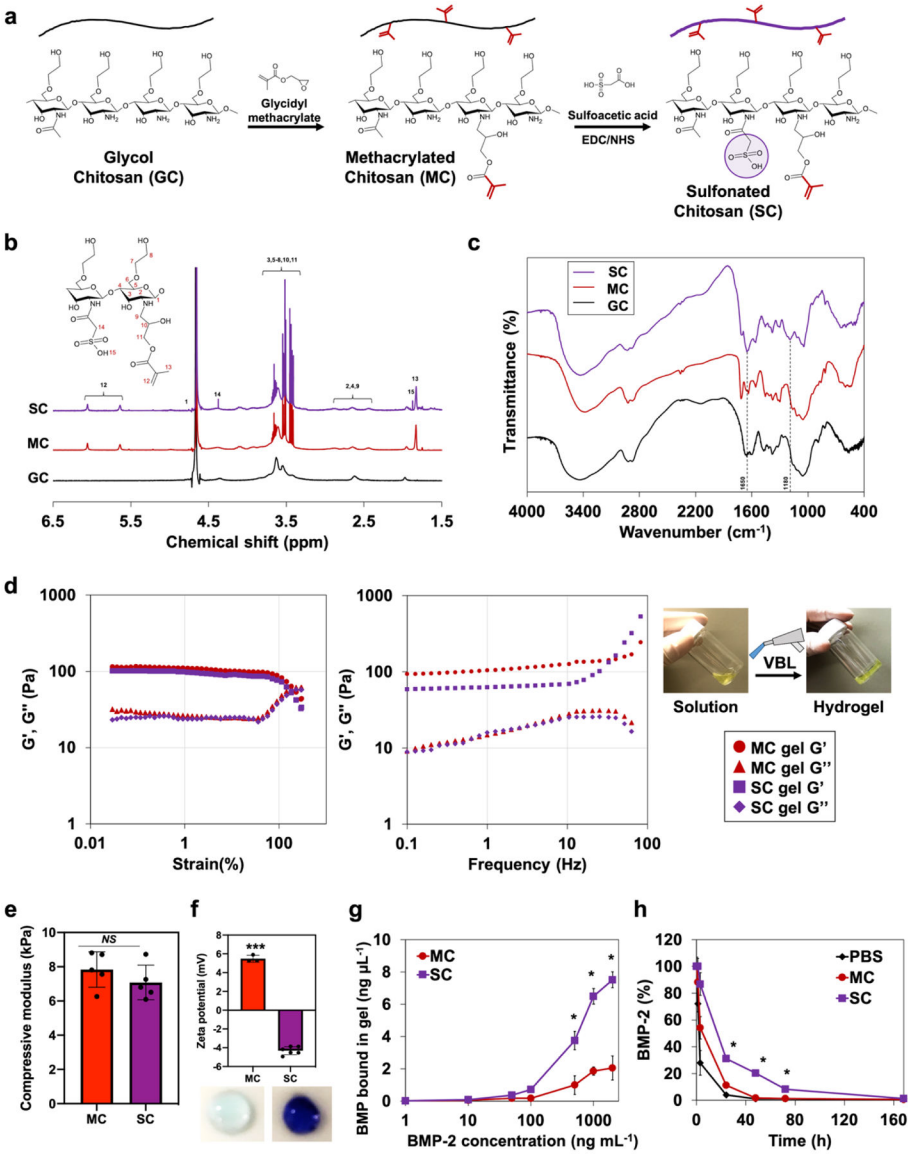

Figure 1.

Characterization of sulfonate hydrogels. a) Reaction scheme of photocrosslinkable sulfonate hydrogel preparation with two-step functionalization (GC, MC, and SC). b) ^{1}H NMR spectra of hydrogel solutions. c) FTIR spectra of hydrogel solutions. d) Rheological properties of MC and SC hydrogels. Monitored storage (G') and loss (G") modulus on strain-sweep (0.02 to 300%, 1.6 Hz) and frequency-sweep (0.1 to 100 Hz, γ = 5.0%) conditions. e) Compressive modulus of MC and SC hydrogels. Error bars indicate standard deviation (n = 5). f) Zeta potential of MC and SC hydrogels. Hydrogels stained with toluidine blue. Error bars indicate standard deviation (n = 6). g) Equilibrium binding isotherms of BMP-2 to MC and SC hydrogels. h) BMP-2 half-life extension in SC hydrogel solution in comparison to MC and PBS. *$p < 0.05$, ***$p < 0.001$, and NS = not significant.

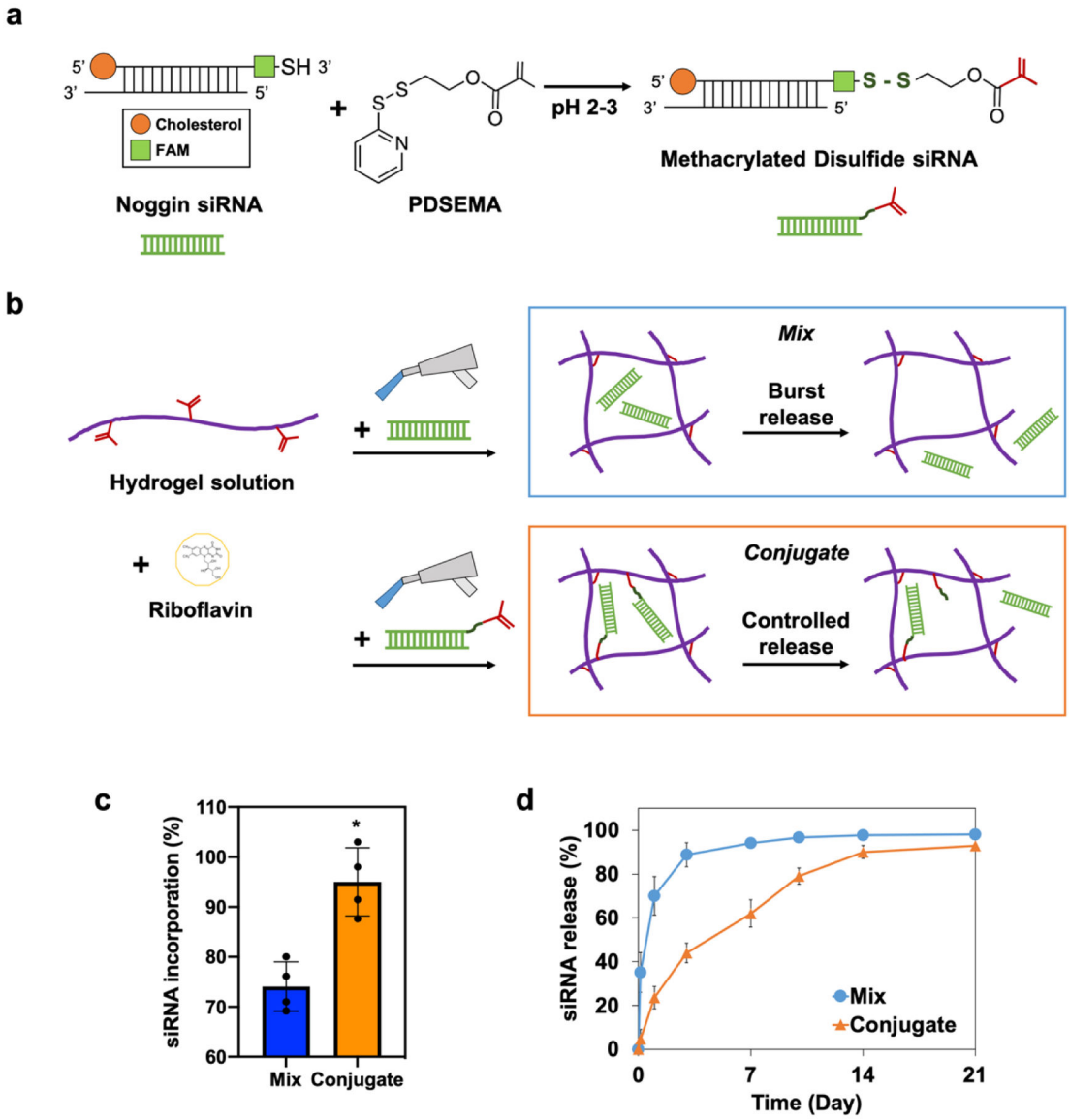

Figure 2.

Preparation of hydrogel-siRNA conjugate. a) Reaction scheme to prepare photocrosslinkable metharylated disulfide siRNA. b) Fabrication of simply mixed and conjugated hydrogel-siRNA by visible-blue-light irradiation. Riboflavin was used as a photoinitiator. Noggin-targeting siRNA was incorporated into sulfonated chitosan hydrogels by simple mixing (Mix) or chemical conjugation (Conjugate). c) siRNA incorporation efficiency of the mix and the conjugate groups. Error bars indicate standard deviation (n = 4). d) Long-term release profile of siRNA from the mix and the conjugate groups for 21 days. *$p < 0.05$.

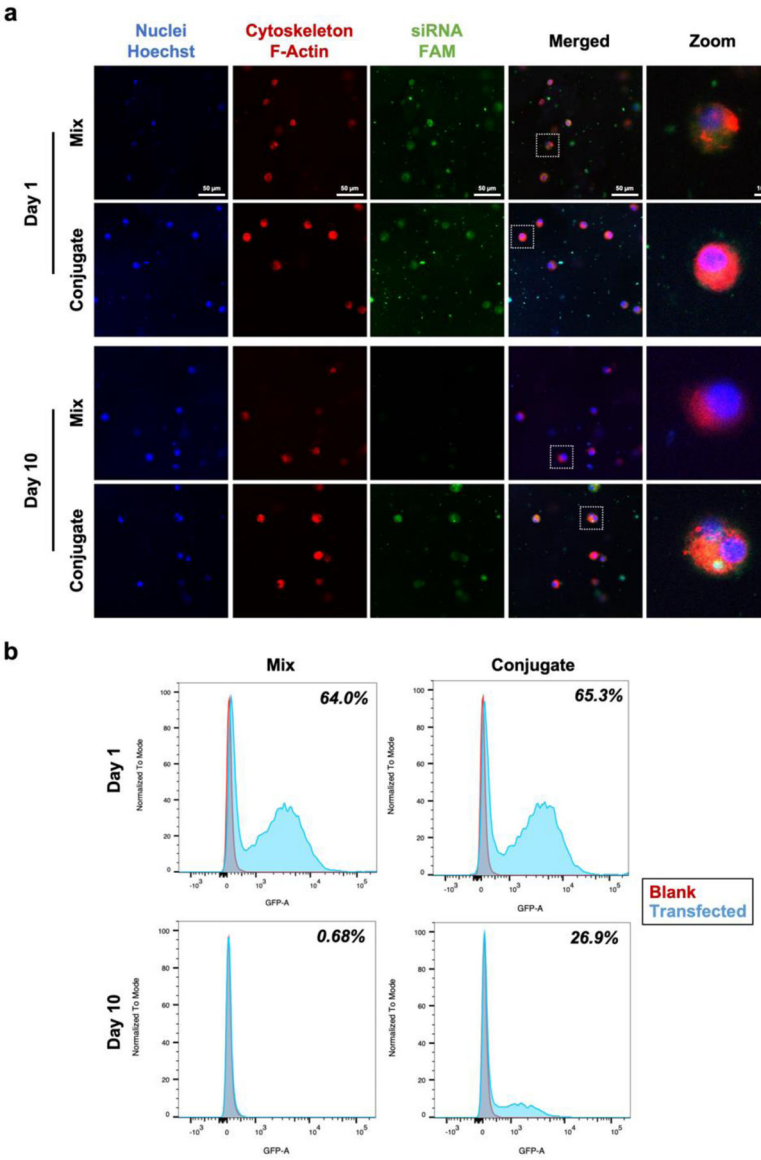

Figure 3.

Cellular uptake of siRNA in hydrogels. a) Representative confocal microscope images of BMSCs encapsulated in sulfonated chitosan hydrogel conjugated with noggin siRNA. Each image shown nuclei (blue), cytoskeleton (red), and siRNA (green). b) Flow cytometry histogram overlaying blank (red) and transfected (blue) cells. BMSCs encapsulated in mixed and conjugated hydrogel-siRNA for 10 days at 37 °C.

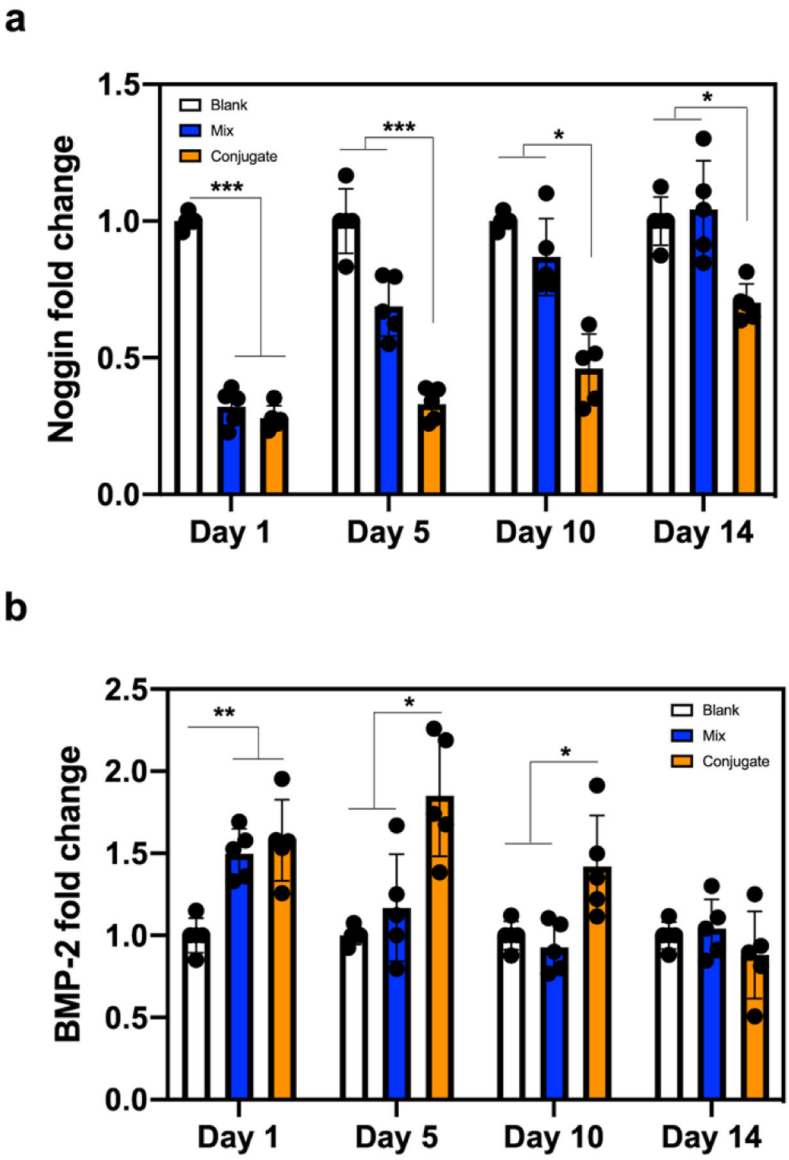

Figure 4.

Gene knockdown efficiency in 3D hydrogels. a) Noggin and b) BMP-2 expression of BMSCs encapsulated in hydrogel-siRNA for 14 days. Noggin-targeting siRNA was incorporated into sulfonated chitosan hydrogels by simple mixing (Mix) or chemical conjugation (Conjugate). Blank is a sulfonated chitosan hydrogel without noggin siRNA. The fold value was normalized with the blank group at each time point. Error bars indicate standard deviation (n = 5). *$p < 0.05$ and ***$p < 0.001$.

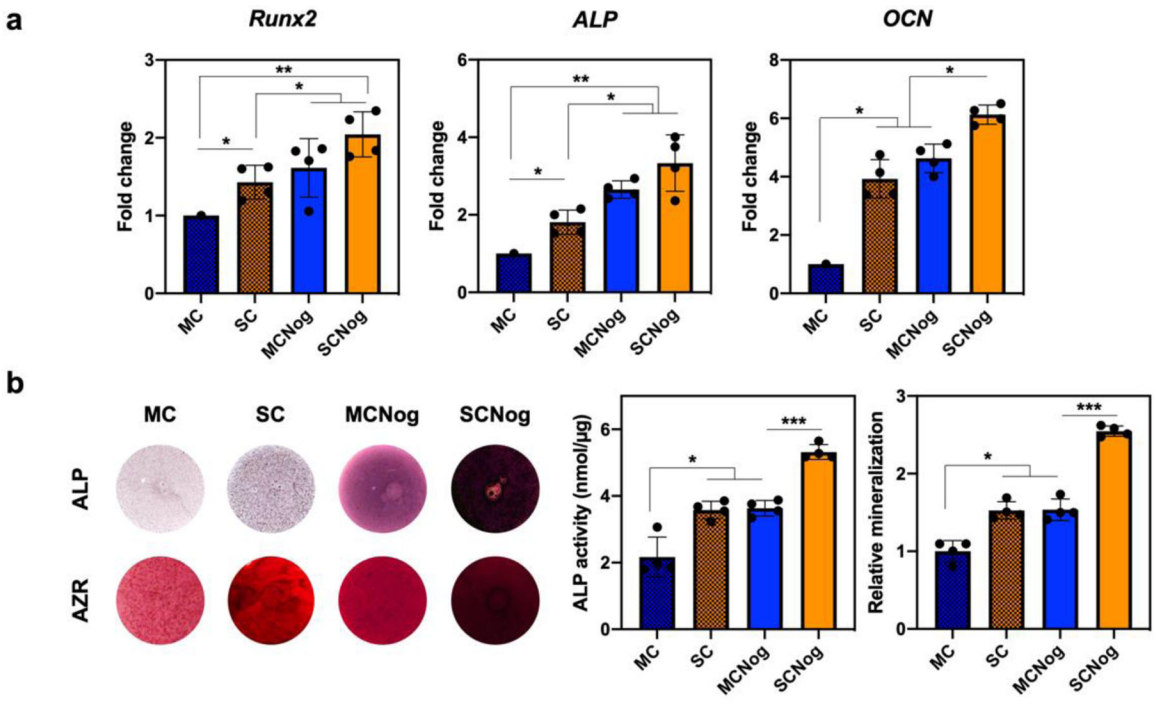

Figure 5.

Osteogenic effect in hydrogel-siRNA. BMSCs were encapsulated into methacrylated chitosan (MC) or sulfonated chitosan (SC) hydrogels conjugated with non-targeting siRNA or noggin-targeting siRNA (MCNog and SCNog). a) Osteogenic gene expression quantified by qRT-PCR at day 4 for *Runx2* and *ALP* and at day 14 for *OCN*. b) ALP and alizarin red S (AZR) staining of hydrogel-siRNA. ALP activity was normalized by total protein expression at day 4 and mineral production was quantified at day 14. Error bars indicate standard deviation (n = 4). *$p < 0.05$, **$p < 0.01$, and ***$p < 0.001$.

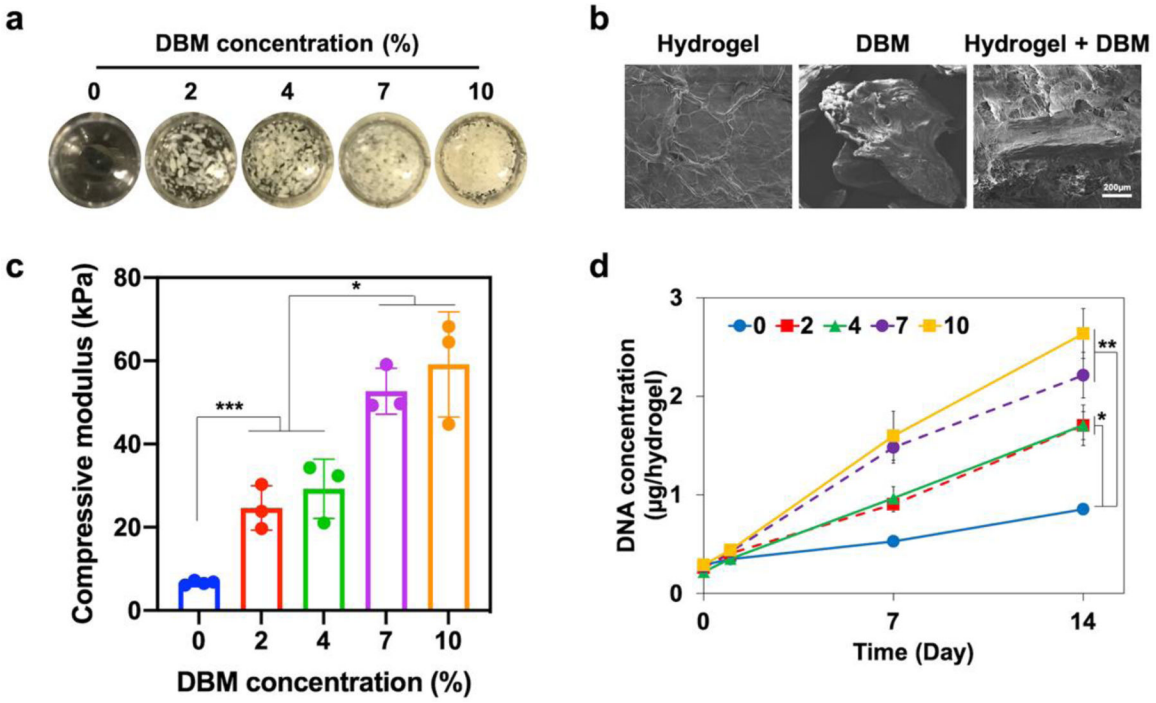

Figure 6.

Characterization of DBM-hydrogel composites. DBM was incorporated into sulfonated chitosan hydrogels conjugated with noggin-targeting siRNA. a) The images of composites with various DBM concentrations (0, 2, 4, 7, and 10%). b) SEM images to display DBM incorporation (7%) in a hydrogel network. c) Compressive modulus of composite hydrogels at various DBM concentrations. Error bars indicate standard deviation (n = 3). d) Growth of BMSCs encapsulated in DBM-hydrogel composites measured by picogreen DNA assay for 14 days. Error bars indicate standard deviation (n = 4). *$p < 0.05$, ***$p < 0.001$, and NS = not significant.

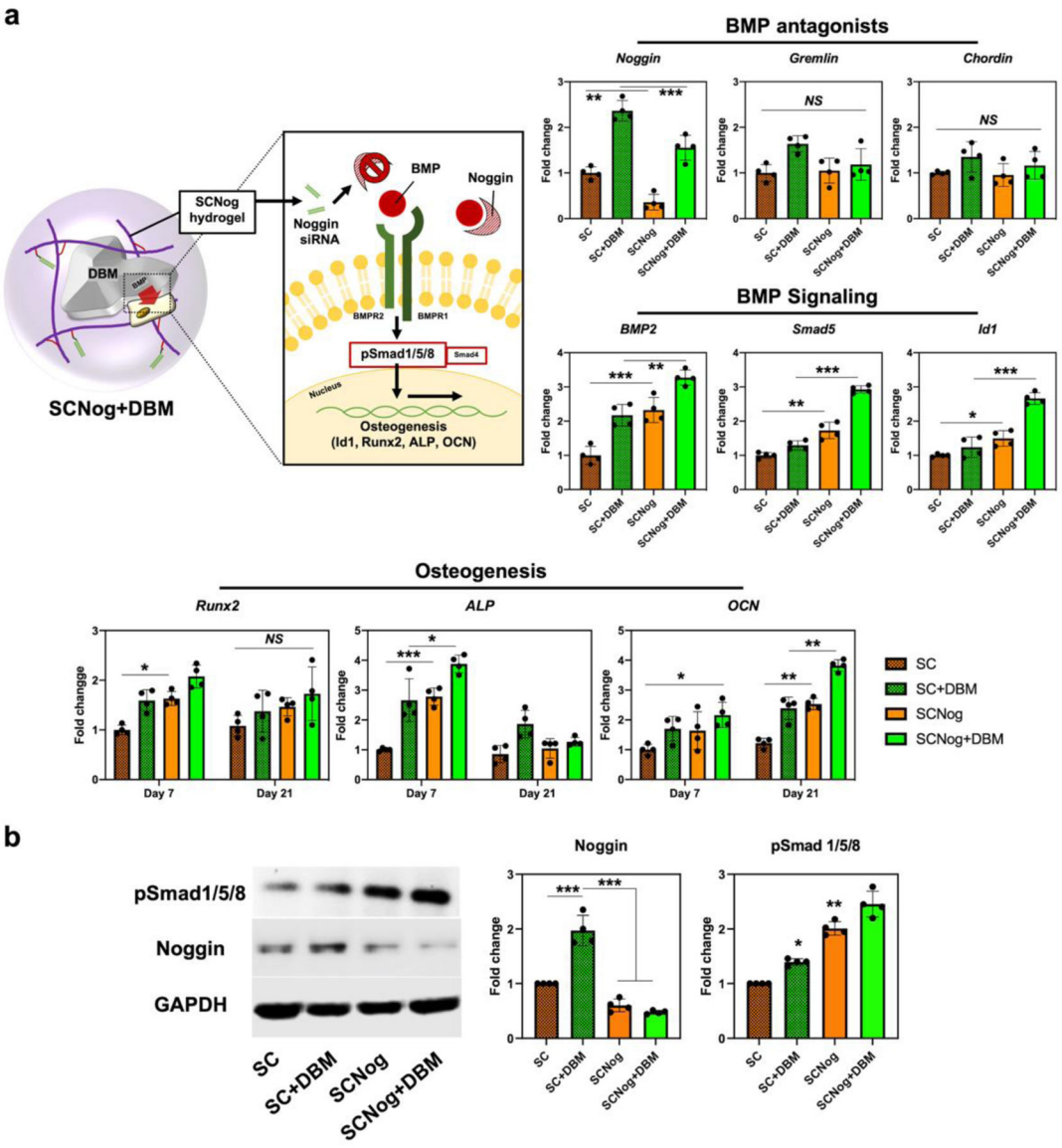

Figure 7.

DBM-hydrogel composite enhancing osteogenesis via BMP signaling activation. a) Schematic illustration of BMP signaling and osteogenic gene expression induced by DBM-hydrogel composite. BMSCs were encapsulated into methacrylated chitosan (MC) or sulfonated chitosan (SC) hydrogels conjugated with non-targeting siRNA or noggin-targeting siRNA (MCNog and SCNog). Gene expression was assessed by qRT-PCR; *noggin*, *gremlin*, *chordin, BMP-2*, *Smad-5*, and *Id-1* at day 4, *Runx2*, *ALP*, and *OCN* at day 7 and day 21. b) Protein expression of GAPDH, noggin, and pSmad 1/5/8 evaluated by western-blot assay. Noggin and pSmad 1/5/8 expression were normalized by GAPDH. The quantification results were analyzed by ImageJ. Error bars indicate standard deviation (n = 4). *$p < 0.05$, **$p < 0.01$, ***$p < 0.001$, and NS = not significant.